EFDA–JET–PR(11)54

I. Bolshakova, A. Quercia, V. Coccorese, A. Murari, R. Holyaka, I. Ďuran,
L. Viererbl, R. Konopleva, V. Yerashok, MSL LPNU Contributors
and JET EFDA contributors

Magnetic Measuring Instrumentation with Radiation-Resistant Hall Sensors for Fusion Reactors: Experience of Testing at JET

Magnetic Measuring Instrumentation with Radiation-Resistant Hall Sensors for Fusion Reactors: Experience of Testing at JET

I. Bolshakova[1], A. Quercia[2], V. Coccorese[2], A. Murari[3], R. Holyaka[1], I. Ďuran[4], L. Viererbl[5], R. Konopleva[6], V. Yerashok[1], MSL LPNU Contributors[7] and JET EFDA contributors*

JET-EFDA, Culham Science Centre, OX14 3DB, Abingdon, UK

[1]Magnetic Sensor Laboratory of LPNU, Lviv, Ukraine
[2]Associazione EURATOM-ENEA per la Fusione, Consorzio CREATE, Napoli, Italy.
[3]Associazione EURATOM-ENEA per la Fusione, Consorzio RFX, Padova, Italy.
[4]Institute of Plasma Physics AS CR, Association EURATOM-IPP.CR, Prague, Czech Republic.
[5]Research Centre Rež, Czech Republic.
[6]Petersburg Nuclear Physics Institute, Gatchina, Russia
[7]Magnetic Sensor Laboratory of Lviv Polytechnic National University, 1 Kotliarevsky, Lviv, 79013, Ukraine
** See annex of F. Romanelli et al, "Overview of JET Results", (23rd IAEA Fusion Energy Conference, Daejon, Republic of Korea (2010)).*

Preprint of Paper to be submitted for publication in
IEEE Transactions on Nuclear Science

ABSTRACT

Research programs for the development and experimental estimation of diagnostics are under way at Joint European Torus (JET) – one of the largest operating fusion reactors. These diagnostics are relevant for solving diagnostic tasks of International Thermonuclear Experimental Reactor (ITER). The paper discusses the principles of designing the magnetic measurement instrumentation based on the application of steady-state radiation-resistant semiconductor Hall sensors. It also presents the results of the instrumentation's application for ex-vessel magnetic field measurement on JET reactor during the latest deuterium campaign, and the prospects of further enhancement in magnetic diagnostic accuracy and reliability. Since neutron fluxes are much larger on ITER, at ex-vessel sensor locations, than those achievable on JET, the sensors have been tested in ITER-relevant radiation environment in nuclear research reactors.

1. INTRODUCTION

Magnetic fields in tokamaks are intended for plasma confinement, hence, magnetic diagnostic is one of the most fundamental measuring systems for magnetic confinement fusion devices. Tokamak efficient operation relies on the accuracy of information provided by magnetic diagnostics required for plasma control in real-rime mode. This being said, magnetic diagnostics should match the complex technical conditions of tokamaks, including radiation loads of neutron and γ-fluxes, increased temperatures, high vacuum, limited access to the diagnostic components for their maintenance. Overall number of magnetic sensors in Joint European Torus (JET) is approximately 500, whereas in International Thermonuclear Experimental Reactor (ITER) the number will reach 1700 and ex-vessel sensors are to be placed in 60 locations in 20 zones. Radiation loads also considerably vary in ex-vessel sensor locations: in JET neutron fluxes are $3 \cdot 10^6$ n·cm$^{-2} \cdot$ s^{-1}, whereas in ITER they will reach from 10^8 n · cm$^{-2} \cdot$ s^{-1} to 10^{10} n·cm^{-2}·s^{-1} [1]. Maximum neutron fluence in ITER is expected to be $F = 1.3 \cdot 10^{18}$ n·cm^{-2} that is four orders higher than fluence in JET during Deuterium-Tritium (D-T) operation [2]. Nevertheless, testing various diagnostics in JET can be of indubitable benefit to ITER, particularly if they are complemented with tests in nuclear research reactors under ITER-relevant radiation conditions.

Magnetic diagnostic system of tokamaks employs mainly inductive sensors of various geometry, both inside (in-vessel sensors) and outside the vacuum vessel (ex-vessel sensors). However, the inductive method, based on pick-up coils and integrators, is prone to the influence of radiation-induced parasitic effects [3] in the conditions of high neutron fluxes during prolonged shots. These parasitic signals, if integrated over long periods, can significantly limit the resulting measurement accuracy to 3.5% [4].

To fight the degradation risk for measurement accuracy, steady-state sensors of magnetic field are introduced into the magnetic diagnostic system of tokamaks by installing them ex-vessel. Several types of steady-state sensors are known, such as sensors on Giant MagnetoResistance (GMR) [5], MicroElectroMechanical Systems (MEMS) [6]. However, currently the most promising devices for increasing the accuracy of magnetic field measuring in long-pulsed fusion reactors like ITER are semiconductor Hall sensors with capacity of direct measurement of both steady-state and high-frequency magnetic fields with wide magnetic flux density (10^{-3}T to 12T) and temperature (4.2K - to 550K) ranges. They are also operable in radiation conditions of high-energy neutron fluxes and fluences, exceeding the maximal level of radiation loads of not only JET, but also ITER. Together with specially developed electronics they make up the magnetic measuring instrumentation capable of solving the complex task of periodic in-situ recalibration, and ensuring long-term measurements without sensors' reinstallation.

In 2005 the prototypes of sensor instrumentation based on Hall sensors and produced at the Magnetic Sensor Laboratory (MSL) of Lviv Polytechnic National University (LPNU) in Ukraine were successfully tested at JET [2]. In view of the results this testing garnered, as well as positive results obtained while testing these devices in radiation environment of nuclear research reactors, the Radiation-hard Hall Probes Project (RHP, 2007-2009) was included into the JET-EP2 Enhancement Programme, approved by European Fusion Development Agreement (EFDA) Steering Committee on 20 July 2005. The project aim was to complement the ex-vessel magnetic diagnostics that exists at JET with a series of probes comprising Hall sensors, so that the results of their testing at JET could also be of use to ITER ex-vessel magnetic diagnostics.

The main institutions involved in the project were:

- *Magnetic Sensor Laboratory*, Lviv, whose tasks included the design and manufacturing of 3D probes with radiation-resistant Hall sensors and electronics, participation in installation at JET, as well as calibration results' analysis;
- *Association ENEA (CREATE)*: leadership of the enhancement project, design and manufacturing of the mechanical supports, integration, assembling and testing, participation in installation at JET, commissioning, analysis and assessment of the signals;
- *Association IPP-CR*: participation in assembly and testing, commissioning, analysis and assessment of the results;
- *JET Operator*: responsible for integration and installation, COntrol and Data Acquisition System (CODAS) interface.

The RHP project took benefit of the combined financial support provided by the European Commission in the framework of EFDA-JET Close Support Unit (CSU) activities and project #3988 of Science and Technology Center in Ukraine (STCU).

2. MAGNETIC MEASURING INSTRUMENTATION: OPERATION PRINCIPLES AND TECHNICAL PARAMETERS

RHP-1 instrumentation for JET magnetic diagnostics produced at MSL contains a 3D probe and control electronics.

Each 3D probe includes: three radiation-resistant Hall sensors, three microsolenoids (inner diameter 2mm) and one thermodiode. Each Hall sensor is located inside the corresponding microsolenoid that generates a magnetic field of certain magnitude. The couple Hall-microsolenoid constitutes an integrated magnetometric transducer (Fig.1). The Hall sensors generate output voltages V_X, V_Y, V_Z, which are proportional to the corresponding components of the measured field B. In calibration mode, the microsolenoids generate the test magnetic field of about 5mT. The test magnetic field produced by the microsolenoid's copper coil does not depend on the radiation dose, and thus can be used for periodic calibration of sensors' sensitivity. The thermodiode allows measuring the probe's temperature, that makes it possible to factor in the effects of temperature drift in Hall sensor and microsoleniod parameters.

Figure 2 shows the 3D probe. Its base and top plate of the lid are produced from anodized aluminium, the lid sides are produced from Rubalit ceramics, which prevents occurrence of eddy currents, and diminishes the lid's screening effect.

The advantage of the instrumentation operation principle is based on the possibility of its periodic calibration without reinstalling the sensors (in-situ calibration). Therefore, the correction of sensors' sensitivity under conditions of their long-term exposure to penetrating radiation is ensured. For such periodic calibration, test field periodically generated in the microsolenoid is used. The methods of signal processing based on synchronous detection allows extracting the small signal of test field 5mT out of the value of the measured reactor field exceeding the test field by a factor of thousand [4].

The developed algorithm of the transduction parameters correction is based on three principles: simultaneous analysis of the transduction parameter by signal's integral and differential components; frequency separation of the signal's integral and differential components; advanced method of transduction function and measured magnetic field calculations. The integral component of the sensor signal is determined by the external reactor magnetic field, and the differential component is determined by the microsolenoid test magnetic field.

Graphic representation of the transduction function and of the measured values is given in Fig.3.

Transduction function is described with a linear equation $V = k \cdot B$, where V – output voltage, B– magnetic flux density (or magnetic induction), k – linear coefficient of sensor signal transduction. The initial transduction coefficient k_0 is determined during the initial calibration process. During the process of operation under radiation conditions this transduction coefficient is drifting and is subject to correction. The correction of the transduction coefficient k_c is conducted by forming the test magnetic field of known value. The test field is formed with the microsolenoid copper coil. It is considered that given the constant value of the current driven through the microsolenoid, the test field is constant, as its value is determined only by the quantity of microsolenoid windings and its diameter. As it is shown in Fig.3, the transduction coefficient k_c is determined by measuring the voltage change value ΔV_c. Thus, in each specific moment of time, having measured the ΔV_c, the transduction coefficient of the output sensor voltage may be calculated as $k_c = \Delta V_c / \Delta B$. Offset voltage drift correction is conducted by cyclic change of current direction through Hall sensors and allows decreasing the absolute error of the magnetic field measuring down to 0.3mT. The error of conversion parameter correction algorithm is 0.1%, as it was observed in experimental research.

The developed method of in-situ calibration has been successfully applied for measuring three orthogonal components B_X, B_Y, B_Z of the magnetic field at JET during the recent deuterium campaign C27. Six sets of magnetic measuring instrumentation PHP-1, each consisting of a 3D probe and a control electronics unit have been spatially located at JET reactor in three areas: the first area (Torus hall) houses the 3D probes at the spots of magnetic field measurement, the second area (Torus hall) contains the electronic units, and in the third area (Diagnostic hall) there is the Cubicle with CODAS control and data acquisition units.

The *3D probes* with Hall sensors have been installed outside the JET vacuum vessel for measuring the ex-vessel magnetic field in a number of spots with certain coordinates. Electronic units have been placed about 2 m away from the probes; signals from the electronic units have been transferred via cables about 100 m long to the data acquisition system.

The *Electronic unit* generates analog differential signals (voltages), which are transmitted via twisted pairs into the respective units (CODAS). Control over the operation modes of the electronic unit is ensured by logical signals generated by JET equipment. The electronic unit can operate in two modes: “Measurement” mode, and “Calibration” mode. In “Measurement” mode, the three components of the field: B_X, B_Y, B_Z are recorded in real time by means of analog-to-digital conversion operating at a standard 5kHz CODAS sampling rate. “Calibration” mode is meant for periodic determination of Hall sensor sensitivity; the sensor parameters in the course of long-term exploitation in radiation environment can slightly drift. This is of principal importance that in “Calibration” mode, the external magnetic field has no effect on differential component of the sensor’s signal. This is implemented by synchronous detectors that separate signals caused by AC test magnetic field of microsolenoid from signals caused by DC external magnetic field [2], [7].

The main technical parameters for RHP-1 magnetic measuring instrumentation:

- Magnetic field measurement ranges: 1) ±2 T; 2) ±0.2T.[1]
- Sampling frequency: 5kHz.
- Error of magnetic field and temperature measurement: 0.3%.
- Maximum probe’s operating temperature: 100°C.[2]
- Maximum survival temperature: 240°C.
- Maximum value of magnetic flux density in electronic unit location area: 0.5T.

RHP-1 magnetic measuring instrumentation generates a set of analog signals, converted thereupon into digital code, and stored in CODAS units. These units also generate the corresponding digital signals used for controlling the operation modes of RHP-1 instrumentation.

In addition, radiation drift of Hall sensor parameters should be minimized to ensure the high accuracy of magnetic field measurement. The application of semiconductor sensors in fusion reactors set forward the requirements concerning their parameter stability in radiation and temperature conditions of these facilities.

Hall sensors’ stability in radiation environment relies on the stability of semiconductor sensor sensitivity ($S = V/B$, where V – output sensor voltage; B – magnetic field value), which first of all

[1] *Field ranges are given for JET. For ITER the magnetic field measurement range can be broadened: from 0.1T up to 5T.*
[2] *Operating temperature is given for JET. For ITER the sensors’ operating temperature can be from 120°C up to 150°C.*

relies on such semiconductor material parameter, as charge carriers concentration (n).

The rate of charge carrier concentration change under irradiation with neutron flux is determined as $\Delta n/\Delta F \approx \alpha - \beta n$, where n – charge carrier concentration in irradiated material, F – fast neutron fluence, α – coefficient of donor (or acceptor) introduction due to nuclear doping, β – cross-section for the generation of acceptor-type (for InSb semiconductor) or donor-type (for InAs semiconductor) radiation defects [8]. For an optimal initial concentration $\alpha \approx \beta n$, that corresponds to $\Delta n/\Delta F \approx 0$, which is prerequisite to sensor's radiation stability.

Thus, the methods of obtaining the radiation-resistant sensors should be aimed at minimizing the change of free charge carrier concentration (n) in semiconductor sensor material. If this condition is satisfied, the change of the sensor's main parameter – its sensitivity (S) – is also minimal, since sensor sensitivity is inversely proportional to charge carrier concentration in sensor material.

It should be taken into account here that minimal change of charge carrier concentration is accumulating, when high neutron fluences are achieved, thus resulting in some drift of the sensor's output signal. To factor this in, and to ensure high measurement accuracy, the electronic methods for in-situ correction of sensor signals during their irradiation with neutron flux described in this paper have been developed.

Technological methods of enhancing the sensors' radiation resistance are based both on the methods of semiconductor sensor materials' chemical doping with a complex of doping impurities (donor, isovalent, rare-earth) up to optimum initial concentration of free charge carriers (n_{opt}), as well as on the methods of their properties' radiation modification.

Sensors used in 3D probes installed at JET were manufactured on the basis of InSb/i-GaAs semiconductor heterostructures. Active elements of the sensors were formed on thin (1μm) doped layers of InSb placed on semi-insulating substrates of GaAs (400μm).

Optimal charge carrier concentration determination in sensor semiconductor material was carried out by experimental investigation of concentration dependence of sensor sensitivity under their irradiation with neutrons in nuclear research reactor IBR-2 (Joint Institute for Nuclear Research, Dubna) in a wide range of neutron fluences from $10^{15}\ n \cdot cm^{-2}$ up to $3 \cdot 10^{18}\ n \cdot cm^{-2}$. Optimal charge carrier concentration in InSb semiconductor material equals $n_{opt} = 6 \cdot 10^{17}\ cm^{-3}$ [8].

It was taken into account here that two mutually compensating processes take place simultaneously in the InSb semiconductor material under irradiation:

(1) generation of acceptor-type radiation defects by fast (E = 0.1 – 14MeV) neutrons in the crystal lattice of sensor material (primary radiation defects – Frenkel pairs as well as radiation defects clusters);

(2) generation of donors due to reactions of transmutation doping under interaction of thermal (E = 0.025eV – 0.5eV), as well as resonance (E = 0.5eV – 1 keV) and intermediate (E = 1keV – 100keV) neutrons with indium atoms of the main material. The reaction results in formation of stannum, which is a donor dopant for InSb:

$$^{115}In(n,\gamma)^{116}In \underset{54\,\text{min}}{\overset{\beta}{\rightarrow}} {}^{116}Sn \qquad (1)$$

Given the optimal composition of semiconductor material, due to the balance between these two mechanisms, and taking into account fast-slow neutron ratio in the flux, the sensor parameter drift during irradiation can be minimized down to the level that is afterwards subjected to correction with electronics and software of magnetic measuring instrumentation.

The work on the creation and testing of radiation-resistant semiconductor materials for sensors became possible thanks to the support granted by a number of STCU and ISTC projects. It also benefited from the participation of the nuclear physicists from Russia and Czech Republic working at well-known nuclear centers of Dubna, Obninsk, Saint-Petersburg and Rež. Over a thousand of sensor samples have undergone testing in nuclear research reactors IBR-2 (Dubna), WWR-M (Saint-Petersburg), LVR-15 (Rež). This joint work has resulted in both theoretical results pertaining to exploring the radiation physical processes taking place in irradiated semiconductors, and practical results in creating the radiation-resistant semiconductor materials for sensors [8, 9].

The experiments carried out in nuclear reactors have confirmed the sensors' operability in neutron fluxes up to the highest fluences $F = 3 \cdot 10^{18}$ $n \cdot cm^{-2}$, that exceed the level of maximum radiation load expected in steady-state sensors' locations at ITER. Moreover, the sensors' sensitivity change when irradiated up to fluences $F = 10^{15}$ $n \cdot cm^{-2}$ is as low as 0.04%, for fluences $F = 10^{16}$ $n \cdot cm^{-2}$ it is 0.08%, and for the highest fluences $F = 10^{17}$ $n \cdot cm^{-2}$ and $F = 10^{18}$ $n \cdot cm^{-2}$ the sensitivity drift is below (5-10)%, which is well amenable to electronic correction.

Figure 4 in a way of example shows the results from one of the most recent experiments on sensor testing in WWR-M reactor at Petersburg Nuclear Physics Institute. Radiation and temperature conditions of this experiment are very close to the environment in ex-vessel sensor locations at ITER.

Reactor neutron flux rate in this experiment was $2.4 \cdot 10^{11}$ $cm^{-2} \cdot s^{-1}$ with maximum fluence $F = 4 \cdot 10^{17}$ $n \cdot cm^{-2}$ at irradiation temperature 110ºC. These fluence and temperature values satisfy the conditions of ex-vessel sensors in ITER. The change in radiation-resistant sensors' sensitivity at maximum fluence did not exceed 5%.

In this experiment the sensor samples under testing were shielded by cadmium screen, as WWR-M and LVR-15 reactors belong to the type of thermal water-water reactors, where thermal neutrons prevail, and the ratio between their flux and fast neutron flux reaches from 10 to 18. Cadmium screens block most of thermal neutrons and make it possible to cut down this ratio to 1.4. However our testing experience has shown that cadmium screens allow resonance and intermediate neutrons through. These neutrons have the capacity to cause transmutation reactions in sensor material similar to ones engendered by thermal neutrons.

IBR-2 fast pulse reactor is better suited for testing sensors in ITER-relevant radiation conditions. The thermal-fast neutron flux ratio in this reactor is 0.77, which is very close to 0.8 – the value typical for thermal-fast neutron flux ratio in ITER ex-vessel sensor locations. Such thermal-fast neutron flux ratio on the outer side of the vessel in ITER is obtained when 14MeV neutron fluxes penetrate the walls of vacuum vessel. As a result, they slow down, and their share in the overall fast neutron flux

(E = 0.1MeV – 14MeV) in sensors' ex-vessel locations does not exceed (3–5)%. Therefore, IBR-2 reactor conditions are suitable for screen-less sensor testing.

Specialized instrumentation and rigs, which allow measuring sensor parameters directly during the irradiation process (on-line measurements), were created for testing Hall sensors in nuclear reactors. The need for creating such an instrumentation is caused by the fact that under high neutron fluences $F = (10^{17}–10^{18})\ n \cdot cm^{-2}$ the level of induced radioactivity becomes so high, that it is impossible to return the activated samples to the Laboratory for metrological measurements.

The instrumentation for conducting such measurements consists of two parts: one part together with the magnetic field source and the investigated samples is placed in the nuclear reactor channel, another one – at the significant distance in the personnel area. As such experiments are long-lasting (from several weeks to several months, the instrumentation reliability is of critical significance. Such measuring in-situ instrumentation that was developed and manufactured at the Magnetic Sensor Laboratory, makes it possible to carry out on-line measurements of semiconductor sensors directly during the process of their irradiation with high accuracy of ±0.1 % up to high fluences $F \approx 1 \cdot 10^{19}\ n \cdot cm^{-2}$ under the increased temperatures $T_{irr} > 100^{o}C$ [10]. Periodic measurement of noises in measuring circuits, level of electromagnetic noises, resistance in signal transmission lines etc. is carried out during on-line studies. Measurement of sensors' temperature is provided for during their irradiation in order to increase the accuracy. The measurement process is fully automated and fulfilled with the help of appropriate software.

3. INSTALLATION OF MAGNETIC MEASURING INSTRUMENTATION IN JET REACTOR

JET is a large and complex machine; installing new instrumentation sets forward integration problems and requires the development of dedicated mechanical support structures, which were designed and implemented by Association ENEA (CREATE). Due to the presence of the remotely powered electronic units in the Torus hall, a dedicated earth scheme was implemented in order to get noise protection and avoid ground loops, and to comply with the safety requirements.

Two assemblies of RHP-1 instrumentation, each including 3 sets of 3D probes with electronics units, were installed on JET before the C27 campaign. They were located in octants 5 and 8 of the reactor in ports 5DLICP and 8DLICP (Fig.5).

The mechanical support structure of the probes is a rectangular section tube, made of epoxy-glass laminates in order to avoid bandwidth-limiting eddy currents and electromechanical stresses. Its lower side is reinforced with steel parts in correspondence with the fixing bracket and of the LEMO connectors. Due to the elongated shape, a high-precision and versatile mechanical design was needed, so as to assure that, during installation, it would be possible to obtain a proper alignment and a suitable position to avoid mechanical tensions. The compact design was also needed, otherwise installation would have been problematic if not impossible.

Figure 6 shows CAD models of the 3D probe, their mechanical supporting structure, and detail view of the site of installation of the probes and electronic units. The assembly of the instrumentation before installation is illustrated in Fig.7. Photogrammetry techniques were used in order to determine the accurate as-installed coordinates of the sensors (Fig.8).

4. RESULTS OF MAGNETIC FIELD MEASUREMENT AT JET DURING THE CAMPAIGN C27 AND THE PROSPECTS FOR ITER

During the 4 month long deuterium campaign C27, all the instrumentation components installed at JET operated without failure. The signals were systematically acquired and integrated into the JET Control and Data Acquisition System (CODAS). The signals acquired during the experimental campaign have been stored in the JET database and are available for post-experiment analysis.

The commissioning activity also included a "functional" commissioning of the new system, aimed at assessing the physical acceptability of the recorded data. Aiming at that, the measured fields were compared with model-based predictions. The good matching observed (Fig.9) in various experimental situations confirms the reliability and correctness of the measurements.

Periodic in-situ calibration of instrumentation was provided for during the measuring process. Calibration error estimates obtained during the instrumentation development has been confirmed within JET experiments during the campaign C27: basing on the data of more than 1500 pulses it did not exceed 0.1% (Fig.10).

However, the accuracy of magnetic field measurement is limited by a number of such factors as, for instance, precision of sensor positioning inside 3D probe (precision of orthogonality maintenance), planar effect in sensors, as well as some mechanical instability of support structures.

The accuracy of magnetic field measurements in present experiment conditions is estimated as 0.3%. However, it can be enhanced by minimizing the indicated factors.

The further magnetic measuring instrumentation accuracy enhancement is planned with the help of:

- employing the precision optical methods of positioning the sensors and 3D probe's construction details;
- creating the technological methods of obtaining very thin semiconductor films for planar effect minimization;
- ensuring the high coordinate structure precision in sensor locations.

The further magnetic measuring instrumentation reliability enhancement is planned with the help of:

- using the cross-calibration while integrating the conventional inductive transducers with Hall sensors that allows excluding microsolenoids used for generating test magnetic field. The microsolenoids are manufactured from multilayer winding of micron-diameter copper conductors using the organic adhesives, which are not very reliable in radiation conditions;
- increasing the temporal stability of 3D probes by optimizing the probe construction elements (compounds, insulation coatings, etc.)

Thus, under the joint use of technological methods of minimizing the radiation drift of sensor output signal and the developed method of its electronic correction, the magnetic measuring instrumentation accuracy in the ITER-relevant environment in ex-vessel sensor locations may be increased up to the required value of 0.1% [11].

CONCLUSION

The results of the enhancement of the magnetic diagnostic system existing at JET are topical both for JET and for ITER. Testing the magnetic measuring instrumentation based on radiation-resistant Hall sensors during deuterium campaign at JET have demonstrated its operability in the reactor environment, and the possibility of further enhancement of magnetic diagnostics accuracy and reliability. The achieved results together with the results of sensor testing in ITER-relevant radiation conditions of nuclear reactors show good prospects for using the magnetic measuring instrumentation for magnetic field ex-vessel diagnostics of ITER-like new generation reactors.

According to the experimental test results the error of instrumentation in-situ calibration is 0.1%, and the accuracy of the magnetic field measuring – 0.3%.

Hall sensor operation temperature satisfies the ITER temperature conditions in ex-vessel sensor locations.

The conducted Hall sensor tests in nuclear reactors up to neutron fluences $F = 3 \cdot 10^{18}\ n \cdot cm^{-2}$ have confirmed their operability under radiation loads exceeding the ITER-relevant radiation conditions.

For ITER-compatibility of the magnetic measuring instrumentation based upon the radiation-resistant Hall sensors a number of steps is needed, including:

- realization of the method of Hall sensor off-set voltage automatic compensation at JET;
- realization of the method of steady-state Hall sensor differential in-situ calibration at JET;
- completing the tests of the developed magnetic diagnostics means in IBR-2 nuclear research reactor, which will be fully run in 2012 after a three-year shutdown for modernization.

ACKNOWLEDGMENT

The success of the fulfilled work was ensured by the support expressed by the European Commission, EFDA and STCU to the international team of institutions from Ukraine, Great Britain, Italy and Czech Republic.

The research team thanks K. Kovarik from Institute of Plasma Physics, Prague, Czech Republic; F. Shurygin, O. Makido and Yu. Zagachevsky from Lviv Polytechnic National University, Lviv, Ukraine; V. Chekanov from the Petersburg Nuclear Physics Institute (Gatchina, Russia) for their contribution in this work.

REFERENCES

[1]. Loughlin M.J. “Nuclear Enviroment at Magnetic Sensor Positions”. IDM Number ITER_D_2F6S7Y (2008).

[2]. A. Murari, T. Edlington, M. Angelone, L. Bertalot, I. Bolshakova, et al. “Measuring the

radiation field and radiation hard detectors at JET: Recent developments" Nuclear Instruments and Methods in Physics Research A. **593**. (2008). 492-504.
[3]. G. Vayakis, T. Sugie, T. Kondoh, T. Nishitani, E. Ishitsuka, M. Yamauchi, et al., "Radiation-induced thermoelectric sensitivity (RITES) in ITER prototype magnetic sensors", Review of Scientific Instruments **75** (10) (2005) 4324–4327.
[4]. G. Vayakis, C. Walker, "Magnetic diagnostic for ITER/BPX plasmas", Review of Scientific Instruments **74** (2003) 2409-2417
[5]. J. Romeo, "Feasibility study of Colossal Magneto Resistive sensors for ITER". TW5-TPDS-DIADEV D2c (2007).
[6]. J. Kyynäräinen, J. Saarilahti, H. Kattelus, A. Karkkainen, T. Meinander, A. Oja, et al., "A 3D micromechanical compass" Sensor&Actuators A: Physical 142 (2) (2008) p.561-568.
[7]. I. Bolshakova, R. Golyaka "Intelligent system of magnetic field monitoring to be used under radiation operating conditions". Proc. 14th European Conference on Solid-State Transducers (Eurosensors XIV). Copenhagen (Denmark). (2000). 755-758.
[8]. I. Bolshakova, R. Golyaka, A. Matkovskyy "Functionally-integrated magnetometric transducer for radiation resistant measuring devices". Book of Abstracts 3rd European Conference on Magnetic Sensors and Actuators. Dresden (Germany). (2000). 199.
[9]. I. Bolshakova, V. Boiko, V. Brudnyi, et al. "The effect of neutron irradiation on the properties of n-InSb whiskers". Semiconductors (Fizika i tekhnika poluprovodnicov). 39(7). (2005). 780-785.
[10]. I. Bolshakova, V. Chekanov, I. Duran, R. Holyaka, et al. "Methods and Instrumentation for Investigating Hall Sensors During Their Irradiation in Nuclear Research Reactors". IEEE Xplore: Advancements in Nuclear Instrumentation, Measurement Methods and their Application, (2010). 1-6.
[11]. J. How "Project Integration Document PID". ITER_D_2234RH Version 3.0 (2007).

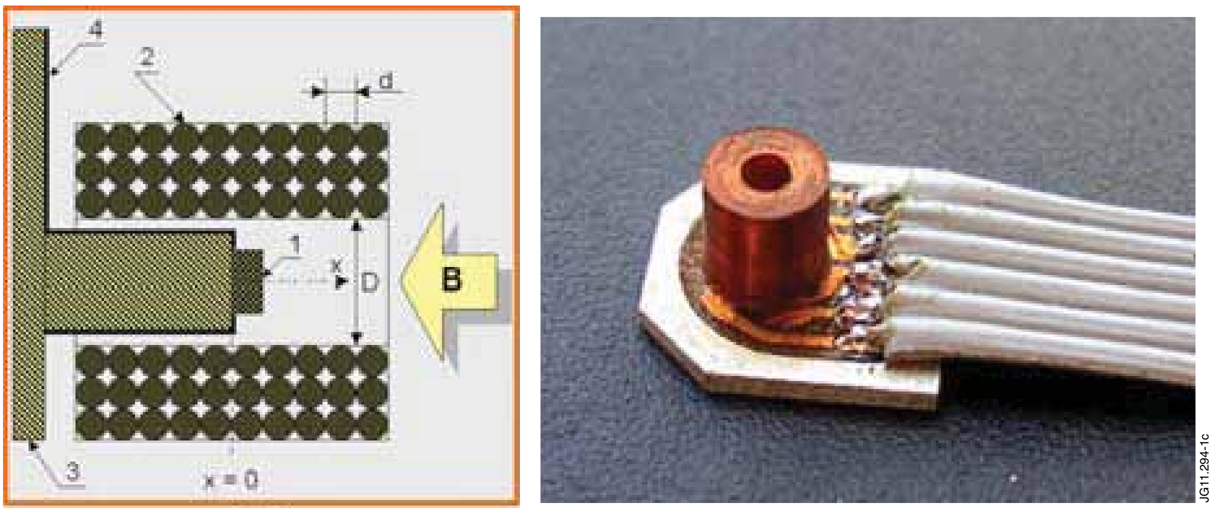

Figure 1: Integrated magnetometric transducer: a) layout (1 – Hall sensor, 2 – microsolenoid's coil, 3 – base, 4 – outputs, D=2mm – microsolenoid's inner diameter, d = 0,05 mm – copper wire diameter, B – magnetic flux density); b) the photograph of 3D probe's assembly.

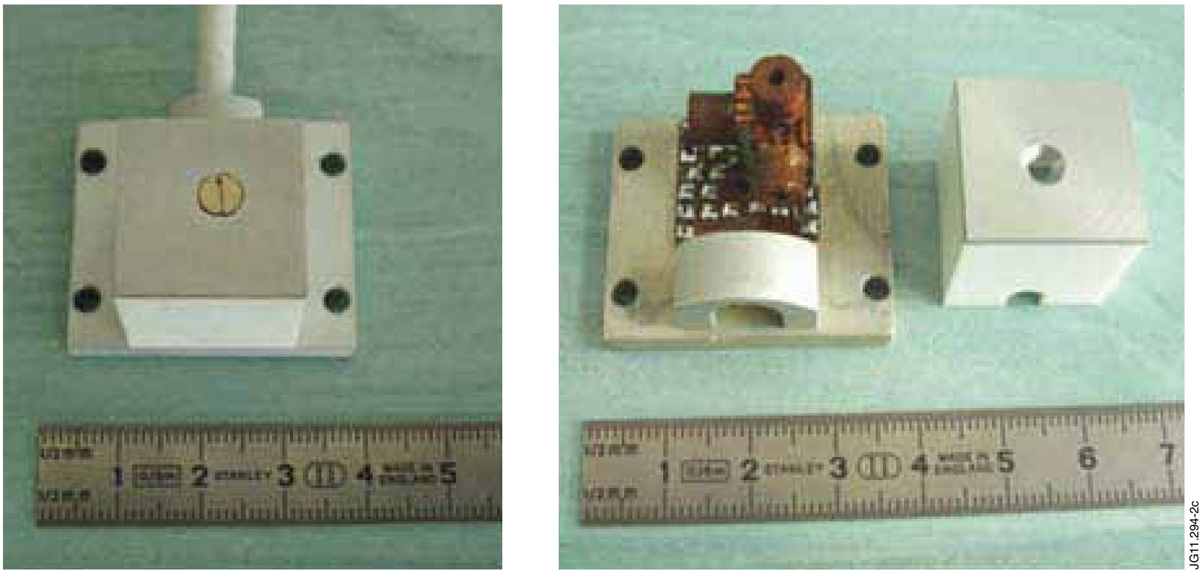

Figure 2: 3D probe's photographs: a) appearance; b) assembly.

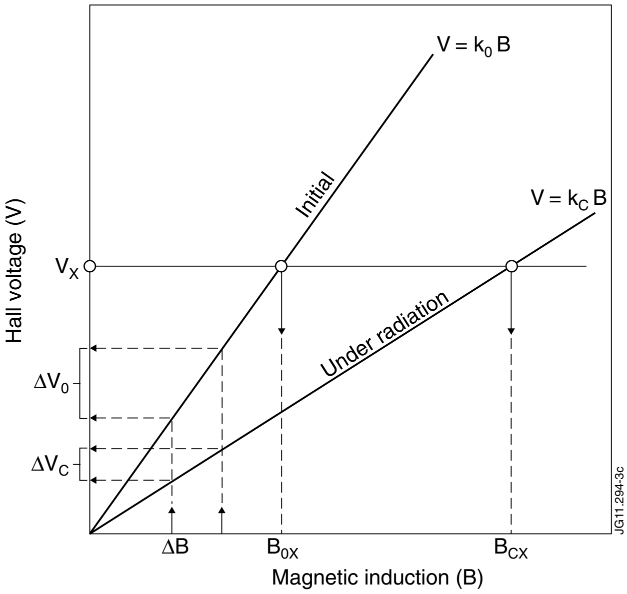

Figure 3: Correction algorithm for the transduction function V_X – measured voltage; k_0 – initial transduction coefficient; k_c – corrected transduction coefficient; ΔB – test magnetic field; ΔV_0 – initial characteristic signal increase; ΔV_c – corrected characteristic signal increase; B_{0X} – calculated value of the initial characteristic magnetic field; B_{CX} – calculated value of the corrected characteristic magnetic field

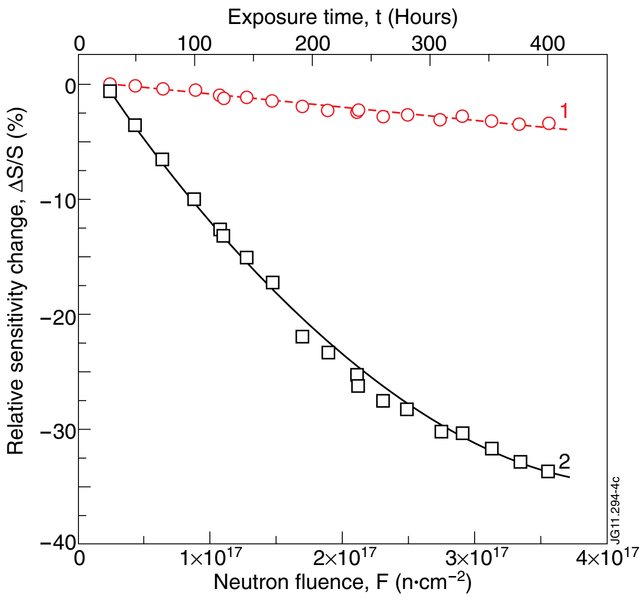

Figure 4: Relative sensitivity change for InSb-based thin-film sensors under the effect of neutron irradiation: 1 – radiation-resistant sensor; 2 – conventional sensor

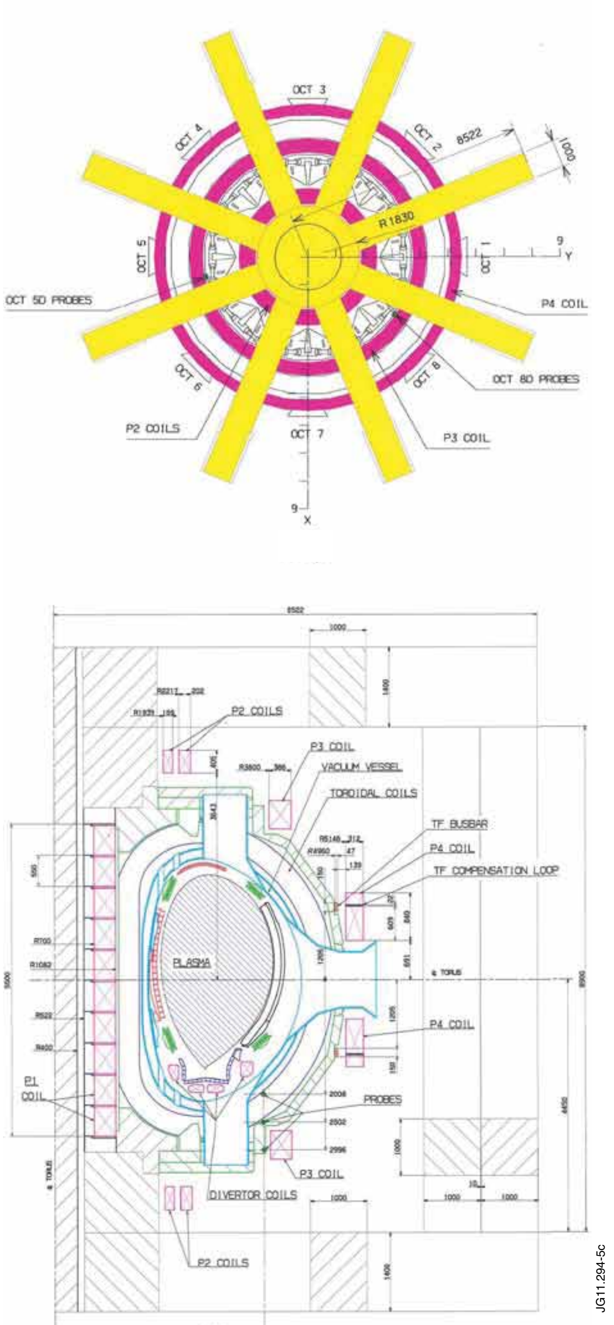

Figure 5: (a) Schematic plan view of the JET machine. The two assemblies, located at octants 5D and 8D, are indicated with small green dots. (b) Simplified cross-section of the JET machine, the location of the three 3D probes is indicated with green dots in the lower-outer part, close to the P3 coil.

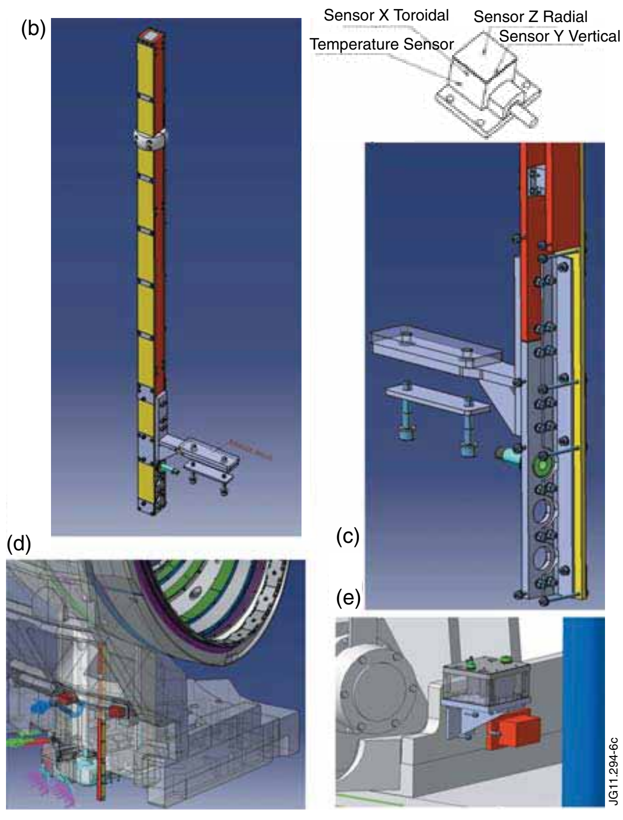

Figure 6: CAD models: (a) the 3D probe; (b) the mechanical support structure for three 3D probes; (c) particular of the internal steel stiffening structure in correspondence of the bracket; (d) the octant 5 vessel and shell (transparent) of JET with the probe's support positioned at sector 5D; (e) the metallic box containing three electronic units located at sector 5E.

Figure 7: Assembly of the magnetic measuring instrumentation (housing, cables and probes support structure).

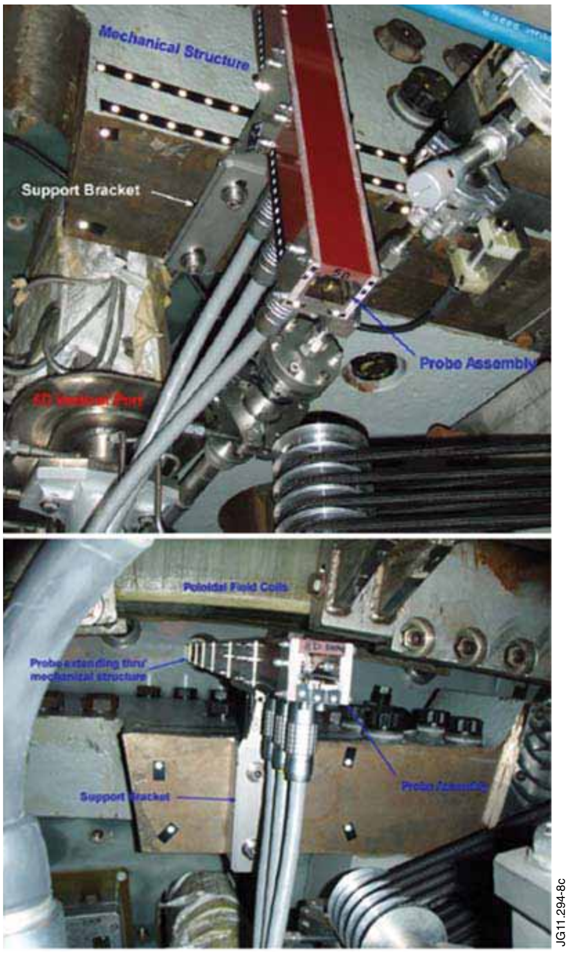

Figure 8: The supporting structures of the probes installed at octants 5D (a) and 8D (b). The black stripes with the reflecting dots stuck to the supports and to the shell of JET are needed for the photogrammetry measurements. The z coordinates of the sensors at octant 8 are about 50mm lowered with respect the ones at octant 5, due to the presence, in octant 8, of a 50mm spacer component inserted between the bracket and the machine.

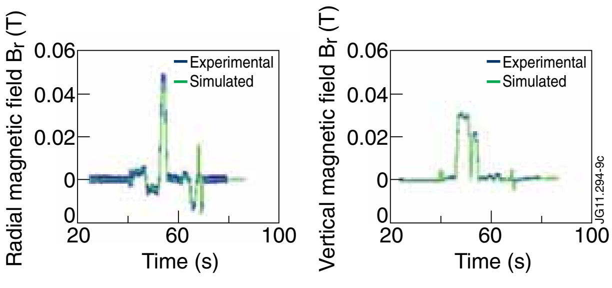

Figure 9: Comparison between the values of radial (a) and vertical (b) components of magnetic flux density vector measured with probe #52, and model calculations in experiment Pulse No: 79206.

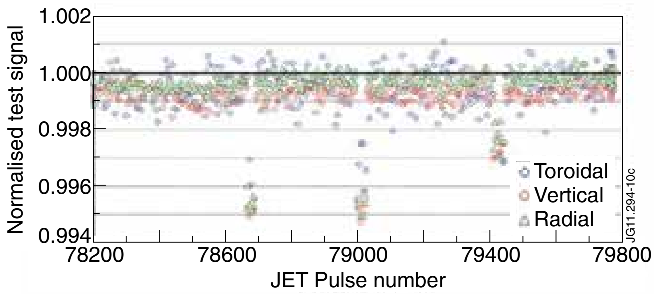

Figure 10: The results of in-situ calibration using the test magnetic field: typical sensor signal deviations do not exceed ± 0.1 %.